Development of Biocompatible Quantum Dots using Zwitterionic Copolymer for Biological Application

Kicheol Yoon

Graduate Program of Chemistry

Ulsan National Institute of Science and Technology (UNIST)

Development of Biocompatible Quantum Dots using Zwitterionic Copolymer for Biomedical Application

A thesis

Submitted to the Graduate School of UNIST

In partial fulfillment of the

Requirements for the degree of

Master of Science

Kicheol Yoon

01. 14 2013 Month/Day/Year of submission

Approved by

_____

Major Advisor

Jongnam Park

Development of Biocompatible Quantum Dots using Zwitterionic Copolymer for Biological Application

Kicheol Yoon

This certifies that the thesis of Kicheol Yoon is approved.

11. 12. 2013 Month

Jongnam Park

signature

_____

HyungJoon Cho

signature

_____

Sebyung Kang

signature

_____

Abstract

Biocompatible inorganic nanomaterial coating of polymer for biomedical application, 2013, Kicheol Yoon, Graduate Program of Chemistry, Ulsan National Institute of Science and Technology (UNIST),

In recent years, zwitterionic polymers has been extensively studied because of their unique water-stability and highly efficient non-biofouling property. This work describes a new class of polymeric ligands for quantum Dot (QD), QDs coated short-chain zwitterionic ligand were stabilized against aggregation from proteins. The zwitterionic polymers are synthesized by reversible addition-fragmentation chain transfer-mediated polymerization to control the uniform molecular weight of random copolymer with histidine group for binding QD surface, and (3-(methacryloylamino)propyl)-dimethyl(3-sulfopropyl)ammonium hydroxide (MPDSAH) group for water solubilization, and primary amine group as binding site for derivatization. Then by carefully handling primary amine of surface, folate-conjugated QDs (QD-FAs) with high photostability are prepared. We demonstrate receptor-mediated conjugation of folic acid functionalized QDs on live cell lines such as Hela cells.

Contents

List of Tables

List of Schemes

List of Figures

List of Abbreviation

AIBN	Azobisisobutyronitrile
CTA	Chain transfer agent
DCM	Dichloromethane
DLS	Dynamic light scattering
DMF	*N,N'*-dimethylformamide
FA	Folic acid
FBS	Fetal bovine serum
FITC	Fluorescein isothiocyanate
LCFM	Laser confocal fluorescence microscopy
MPDSAH	(3-(methacryloylamino)propyl)-dimethyl(3-sulfopropyl)ammonium Hydroxide inner salt
MW	Molecular weight
NHS	N-Hydroxysuccinimide
NMR	Nuclear magnetic resonace
OEG	Oilgo ethylene glycol
PC	Phosphorylcholine
PEG	Poly(ethylene glycol)
PBS	Phosphate-buffered saline
PS	Penicillin/Streptomycin
QD	Quantum dot
RAFT	Reversible addition-fragmentation chain transfer
SLS	Static light scattering
THF	Tetrahydrofuran
TEM	Transmission electron microscopy
TLC	Thin-layer chromatography

Development of Biocompatible Quantum Dots using Zwitterionic Copolymer for Biological Application

1. Introduction

Semiconductor and metallic Nanoparticles (NPs) for application of biomedical imaging have led to considerable advances in diagnosis and therapy. Because first, they have unique optical and electronic properties and second almost all of the disease processes take place on this length scale.[1]

Especially Quantum dots (QDs) are a powerful nanomaterial of photostable fluorophores exhibiting high quantum yields with narrow tunable emission wavelengths through visible and near-IR spectra.[2-6] QD's structures are made up two or more closely positioned quantum dots. One quantum dot has a properties like atom. That means, when the quantum dot is atom level, they don't indicate the specific properties. But when the molecular level, they have unique properties. These properties whose brightness and stability when the cellular imaging at single molecule level are paramount to typical dye and fluorescent protein imaging materials make QDs attractive tools for application of biological labeling and optical fluorescent imaging.[7-9] Nevertheless, the widespread use of QDs in live cell are challenges because of need to five essential QD properties for fluorescence labeling in live cells: small size, high stability (both over time and in a wide pH range), high quantum yields, facile derivatizabilty, and low nonspecific binding.[2] In this study, we have search for enhanced simple chemical methods to functionalize NPs in aqueous condition to invent outstanding material systems for studying biological phenomena.[10]

Most popular non-biofouling materials such as poly(ethylene glycol) (PEG) or oligo(ethylene glycol) (OEG) that via grafting surface of nanoparticles widely used to prevent the adsorption of proteins and cells in aqueous solution.[11-21] However, For long-term applications, PEG is hypersensitive to oxidation damage and does not completely eliminate protein adsorption.[22-28] A steric exclusion effect and hydration are considered as one of the reasons for long PEG polymers to resist nonspecific protein adsorption.[28-30] The existence of water molecules within the PEG layers is required for protein resistance,[28, 31] at least 2-3 molecules of water per ethylene glycol unit and up to a maximum of 10 molecules required for hydration.[20, 28] In addition, the stability of PEG is adjusted to presence of oxygen and transition metal ions because of oxidation,[31, 32] and even though it is able to hinder protein adsorption at room temperature, its non-biofouling properties are diminished above 35 ℃.[32, 33] Phosphorylcholine (PC)-based polymer make up the majority of typical mammalian cell surface and are known to be effective in reducing the adsorption of protein.[32, 34] The zwitterionic phospholipid are constituent of the cell membranes, and have remarkable nonthrombogenic property.[11, 35] Other zwitterionic groups, such as carboxybetaine and sulfobetaie polymer, have recently been studied because of their water-solubility and biocompatibilities and showed non-biofouling property.[11, 36, 37, 38]

Based on the previous report, We synthesized random copolymers with Histamine acrylate, (3-

(methacryloylamino)propyl)-dimethyl(3-sulfopropyl)ammonium hydroxide inner salt (MPDSAH) and PEG acrylate for QD binding, water solubilization, and functionalization, respectively via Reversible Addition-Fragmentation Chain Transfer (RAFT). For this study, Poly(amino-PEG_3)10%-Histamine50%-MPDSAH40% and Poly(amino-PEG_3)25%-Histamine50%-MPDSAH25% was synthesized respectively, and We compare 10% and 25% functional amine to confirm by probing the free amine in the polymer before and after the conjugation using Fluorescein isothiocyanate (FITC), an amine-reactive fluorogenic probe.[39]

We demonstrate extremely low nonspecific binding on protein and high stability exceptional other defect and long lifetime emitting fluorescence, to confirm optical live cell imaging.

2. Results and Discussion

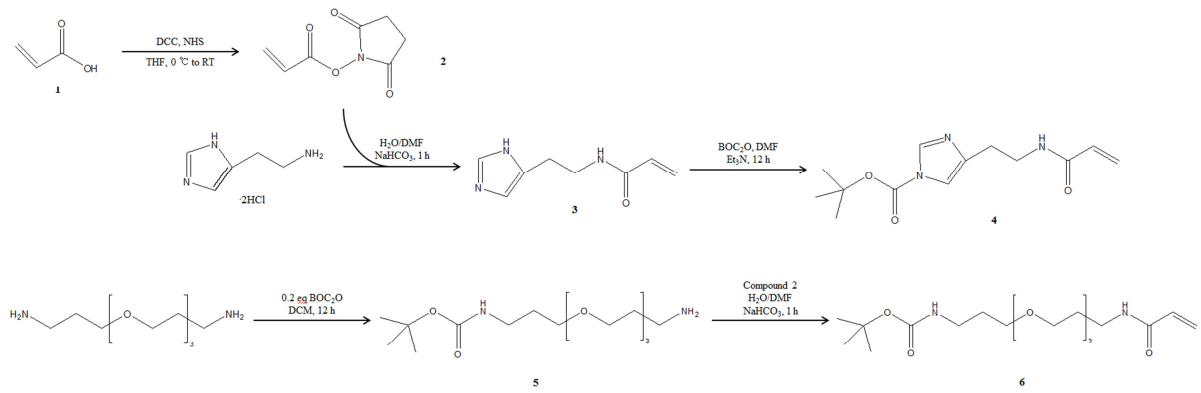

Scheme 1 Synthesis of monomer.

Synthesis of monomer. Scheme 1 indicate the synthesis of monomers for QD binding and derivatization that were used for polymerization. Acrylic acid (1) is connected to primary amine of histamine by amide bond forming reaction. First, NHS-ester of acrylic acid (2) was prepared by coupling reaction at 4 ℃ for 30 min. The resulting product was confirmed by TLC with comparing starting materials. The primary amine of histamine containing imidazole group that is QD binding site was reacted with NHS-ester of acrylic acid to yield monomer (3) because the N-Hydroxysuccinimide (NHS) is used as an activating reagent for carboxylic acids. The imidazole nitrogen of final monomer (4) was protected by BOC group because, when polymerization reaction by using trithiocarbonate RAFT agent, the RAFT agent is highly sensitive to amine group toward degradation by aminolysis. Likewise, monomer (6) was synthesized initially by BOC protected terminal amines and followed by reaction with (2).

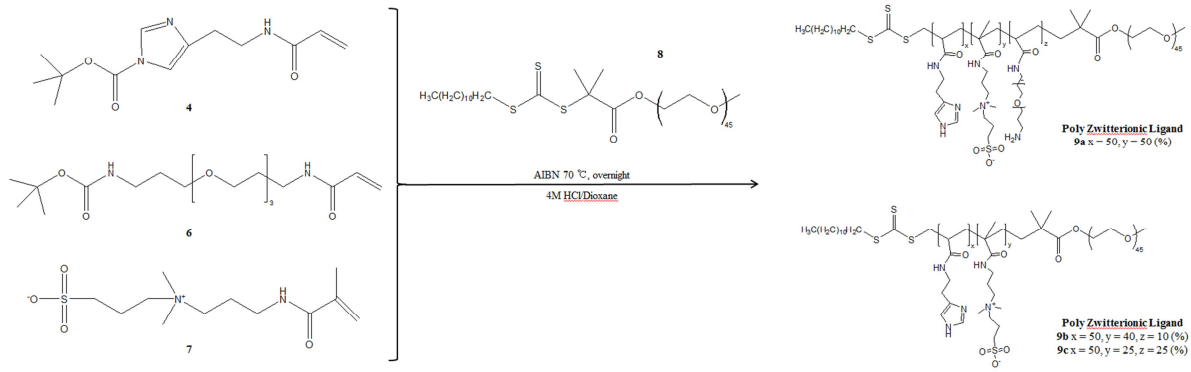

Scheme 2 Synthesis of Polyzwitterionic Ligand (PZL) by RAFT copolymerization.

Synthesis of zwitterionic random copolymer containing imidazole. For the polymerization of 4, 6, 7 (Table 1), we adopted a RAFT polymerization method using the trithiocarbonate chain transfer agent CTA-1 (8) (Scheme 2). Under the standard conditions ([CTA]:[Monomer]:[AIBN] = 1:56:0.2) in methanol (MeOH) at 70 °C in a closed reaction ample. The resulting polymer MWs (9a) were ~ 28 kDa with RMS Error 1.11 e-04 as measured by SLS.

Ligand exchange of QD-PZL. Ligand exchange of 605 nm emitting QDs, CdSe/CdZnS core/shell[2] using polyzwitterionic ligand was performed by displacing the part of imidazole groups which can be binding interaction with the Zn and Cd rich surface of QDs. The ligand exchange conditions were relatively mild and, entailed stirring a mixture of QDs and polyzwitterionic ligand in a solvent of chloroform and methanol mixture at 50 ℃ (Scheme 3). The QD-PZLs were dispersed in water or PBS and then more purified by filter.

Table 1 Nomenclature of polyzwitterionic ligand used compound.

Nomenclature for PZL	Composition in polymer ligand by mole %
PZL	50% cmpd 4/ 50% cmpd 7
$PZ(aminoPEG_3)_{10\%}$	50% cmpd 4/ 10% cmpd 6/ 40% cmpd 7
$PZ(aminoPEG_3)_{25\%}$	50% cmpd 4/ 25% cmpd 6/ 25% cmpd 7

[a] Polymer structure can be found in Scheme 1.2.

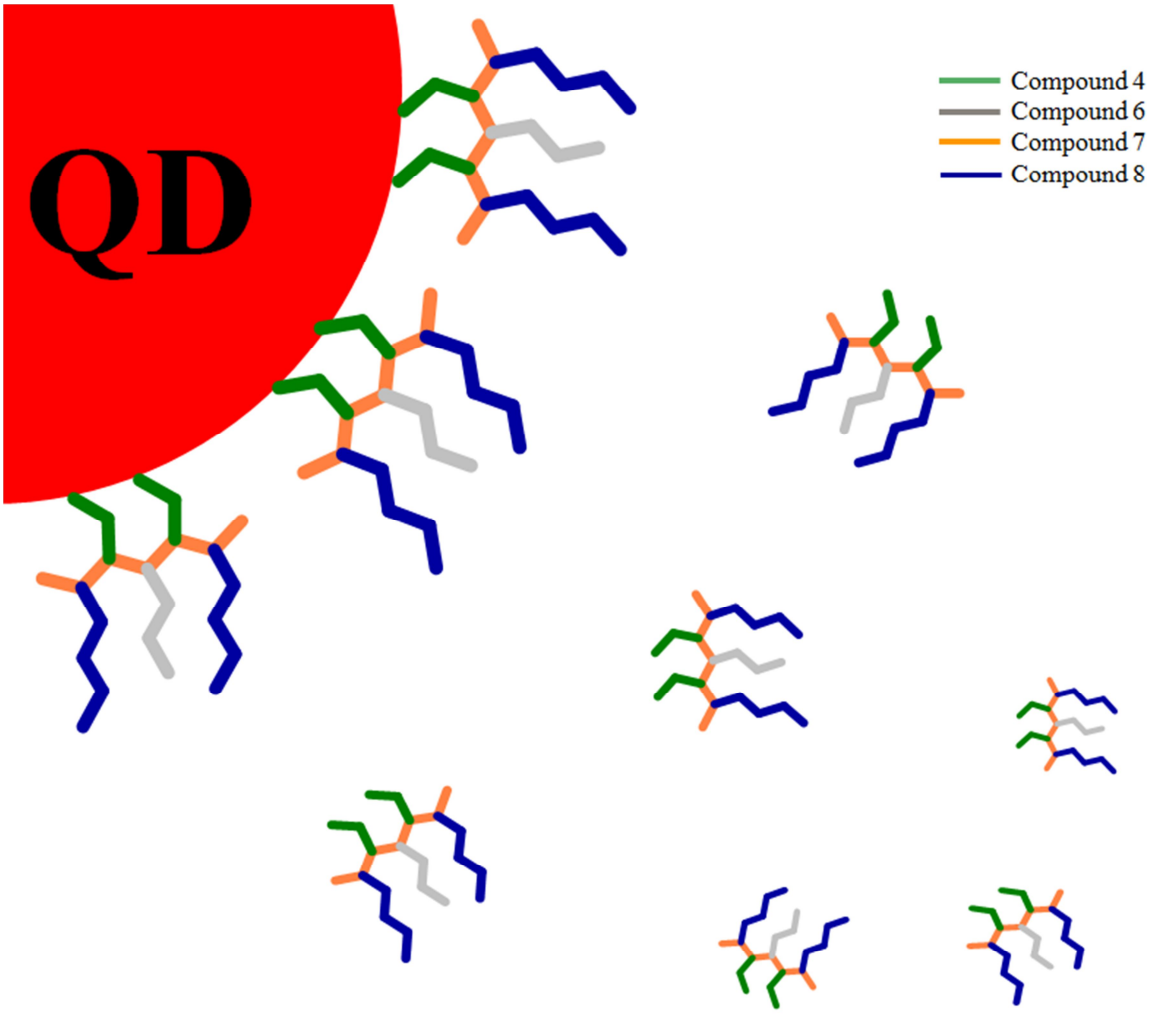

Scheme 3 Ligand exchange of QD by polyzwitteronic ligand.

UV spectra measurement. The Absorbance peak of QD-PZL, QD-PZ(aminoPEG$_3$)$_{10\%}$ and QD-PZ(aminoPEG$_3$)$_{25\%}$ exhibited slight red-shift (Table 2). The fluorescence also was designated other place (figure 1).

Table 2 QD UV spectra as a % amine function in polymer.

QD sample	Absorbance (nm)	Fluorescence (nm)
QD	601	605
QD-PZL	598	613
QD-PZ(aminoPEG$_3$)$_{10\%}$	596	611
QD-PZ(aminoPEG$_3$)$_{25\%}$	595	604

[a] Comparison of absorbance spectra peaks and fluorescence peaks before/after coated polyzwitterionic polymer of various compositions.

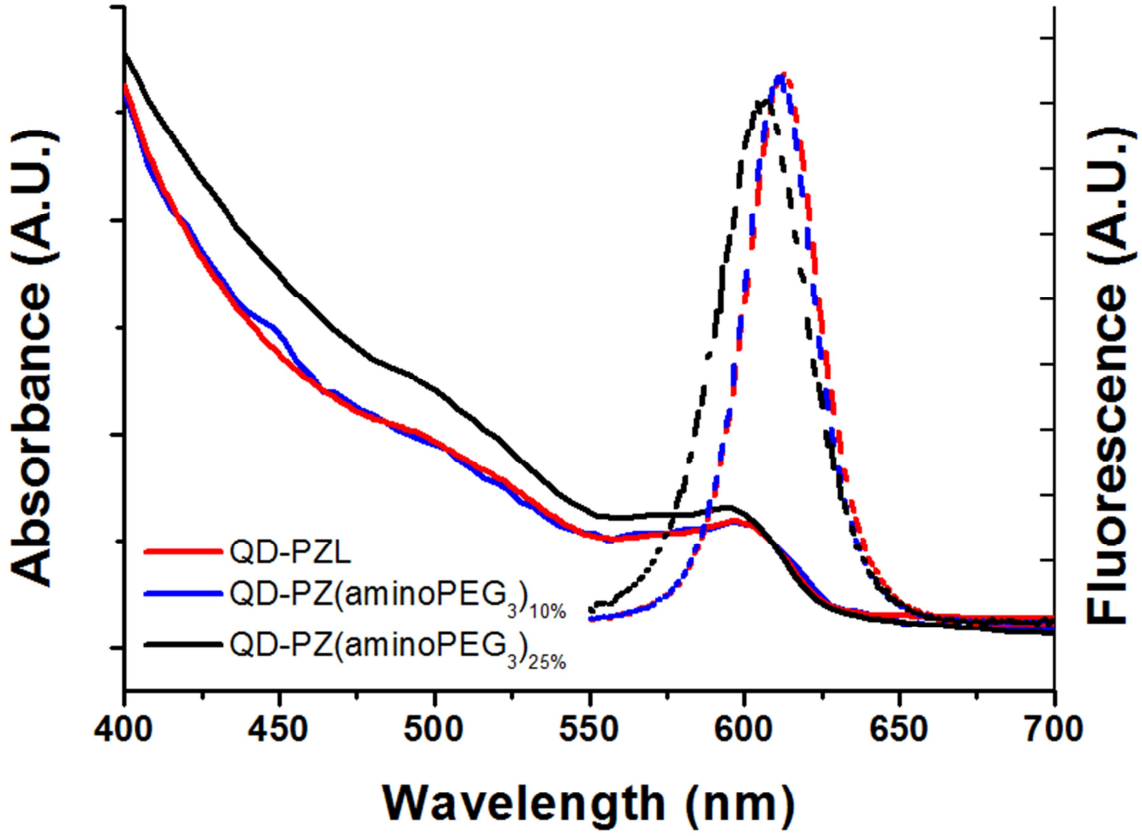

Figure 1 Absorption spectra QD-PZL (— red), QD-PZ(aminoPEG$_3$)$_{10\%}$ (— blue), QD-PZ(aminoPEG$_3$)$_{25\%}$ (— Black) and emission spectra QD-PZL (--- red), QD-PZ(aminoPEG$_3$)$_{10\%}$ (--- blue, QD-PZ(aminoPEG$_3$)$_{25\%}$ (--- black) of QDs after ligand exchange in water, showing a slight shift in fluorescence intensity to depend on the functional modified ligand.

Water-stability measurement by DLS and TEM. QD-PZLs size distributions were imaged by DLS. QD-PZL particle size was around 7.877 nm without showing other specific peak. QD-PZ(aminoPEG$_3$)$_{10\%}$ and QD-PZ(aminoPEG$_3$)$_{25\%}$ was measured at the next step. Each particle size was measured as 10.19 nm and 26.75 nm respectively. The particle sizes were increased with amount of amine part without regularity. And we measured DLS of QD-PZ(aminoPEG$_3$)$_{10\%}$ and QD-PZ(aminoPEG$_3$)$_{25\%}$ one more time after conjugating folic acid. Because we hypothesize that the functional amine aggregated each other particles. So we demonstrated mechanism of functional amine on the surface of QDs by protected functional amine used folic acid. Folic acid conjugated QD-PZLs size distribution was indicated about 7.99nm and 17.39 nm respectively. In the result, the folic acid conjugated QD-PZLs were indicated to decrease the particle size less than QD-PZ(aminoPEG$_3$) without folic acid. We concluded that functional amine affect the aggregation between particles (Figure 2A). The stability of QD-PZLs are well dispersed in water and PBS (Figure 2B). TEM analysis of QDs after ligand exchange with polyzwitterionic ligand shows that QDs are well dispersed. (Figure 2C).

Amine assay analysis by UV. To know how many amine functional groups surround per each QD surface, we used UV-vis (Wavelength ranges : 175~3,300nm, limit resolution : < 0.048 nm) to confirm amine assay. Fluorescent dye FITC was used to the derivatization of amine groups. We measured absorbance about three cases, QD-PZ(aminoPEG$_3$) before derivatization, and QD-FITC mixture, and QD-FITC after filter. The number of working FITC was calculated by comparing the increased absorbance intensity of filtered QD-FITC from pure QD-PZ(aminoPEG$_3$) absorbance. We confirmed 38, 47 amine functional groups per particle were attached to per each QD-PZ(aminoPEG$_3$)$_{10\%}$ and QD-PZ(aminoPEG$_3$)$_{25\%}$ respectively.

Zeta potential analysis. We used zeta potential measuring system (220V, 60Hz)to observe particle aggregation. Our particles have negative charge when it dispersed in water. In general case, particles were said to stable when the magnitude of zeta potential was more than 20 mV. Before adding amine, QD-PZLs had -24.8 mV zeta potential which means well dispersed in water. And zeta potential was tend to increase with adding amine part in polymerization step. After adding 10 % mole percent amine part, zeta potential was increased to -12.6 mV. And at 25 %, zeta potential was -5.0 mV (Figure 4). We can confirm amine parts enhanced aggregation of particles.

pH stability. To find suitable pH for stability of dispersed QD-PZL in water, DLS of particles comparing with QD-PIL[2] were measured. As shown in Figure 5, the QD-PIL had increase size at pH lower than 5, whereas the QD-PZL had linear size without variation in the whole pH range.

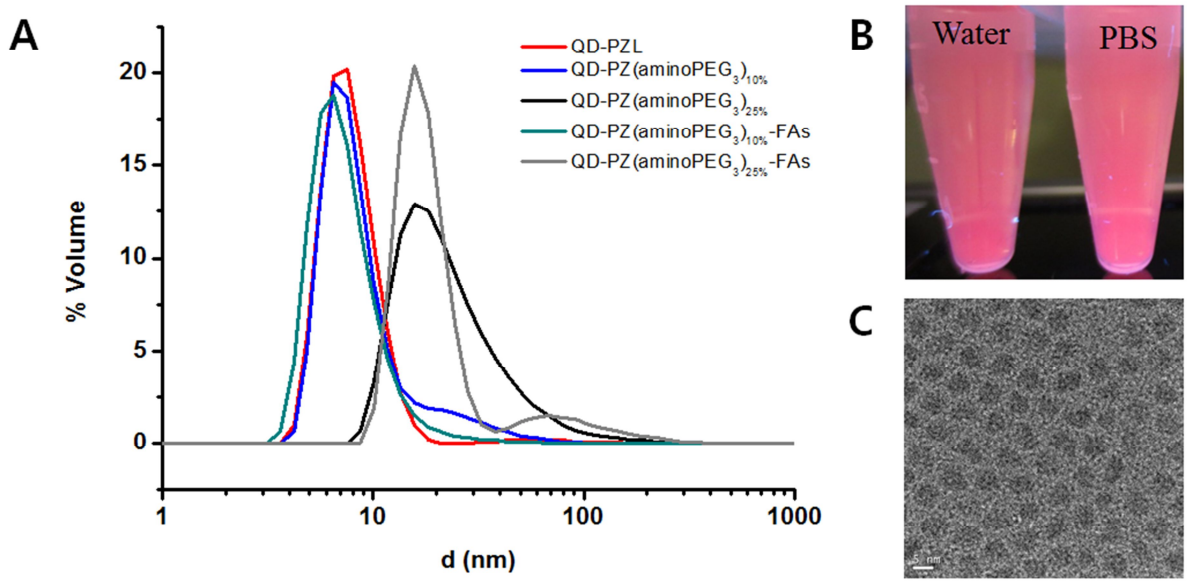

Figure 2 Size analysis of polyzwitterionic QDs. (A) Dynamic light scattering of QD-PZL (— red), QD-PZ(aminoPEG$_3$)$_{10\%}$ (— blue), QD-PZ(aminoPEG$_3$)$_{25\%}$ (— black), folic acid conjugated QD-PZ(aminoPEG$_3$)$_{10\%}$ (— cyan), folic acid conjugated QD-PZ(aminoPEG$_3$)$_{25\%}$ (— gray). (B) Dispersion of QD-PZLs in water and PBS. (C) TEM of polyzwitterionic ligand exchanged QDs, showing monodisperse QD-PZL.

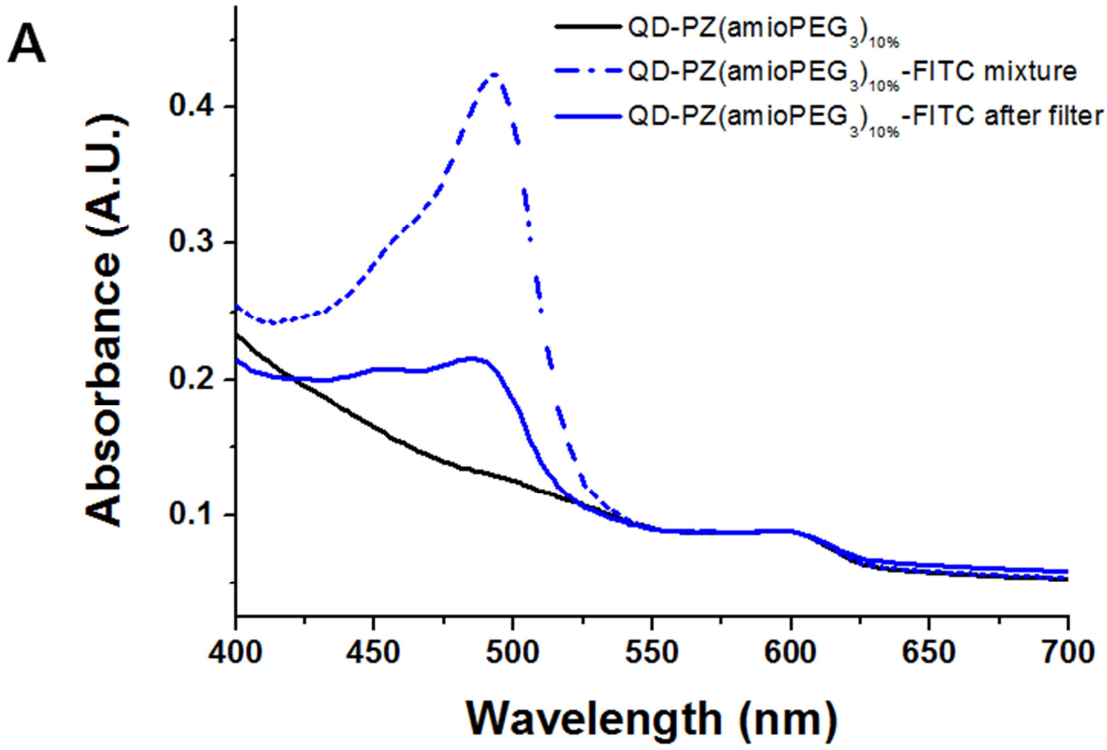
A
QD-PZ(amioPEG3)10%
QD-PZ(amioPEG3)10%-FITC mixture
QD-PZ(amioPEG3)10%-FITC after filter
Absorbance (A.U.)
0.1
0.2
0.3
0.4
400
450
500
550
600
650
700
Wavelength (nm)

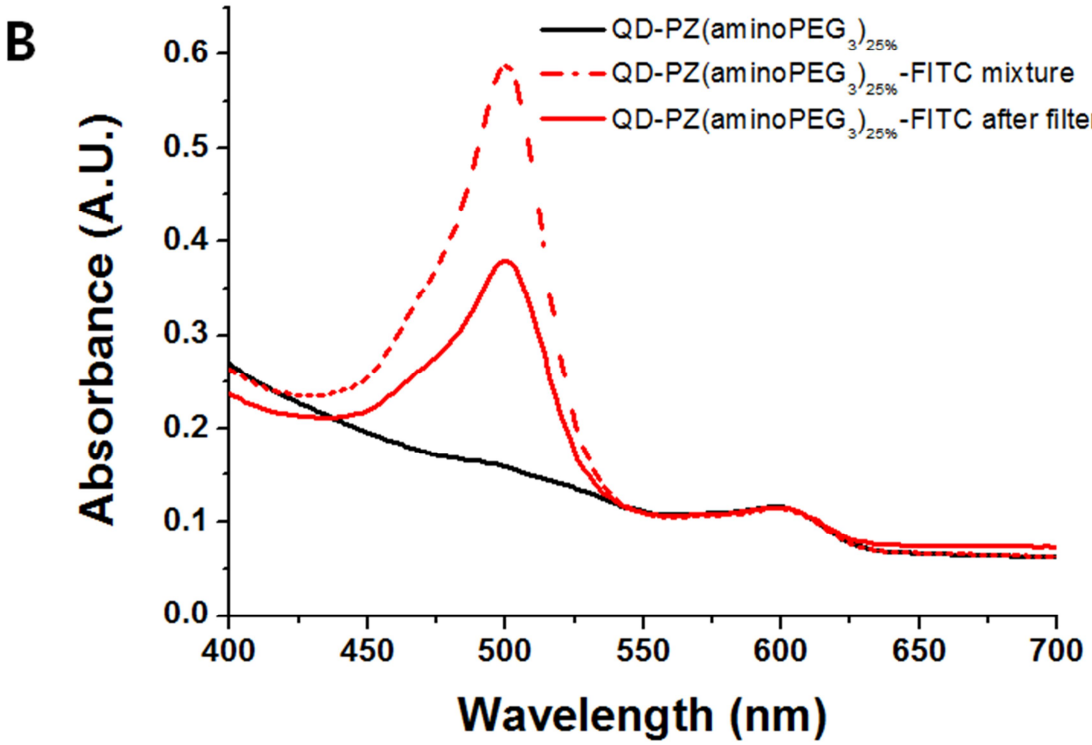
B
QD-PZ(aminoPEG3)25%
QD-PZ(aminoPEG3)25%-FITC mixture
QD-PZ(aminoPEG3)25%-FITC after filter
Absorbance (A.U.)
0.0
0.1
0.2
0.3
0.4
0.5
0.6
400
450
500
550
600
650
700
Wavelength (nm)

Figure 3 Derivatization of amine functional QD-PZL with the fluorescent dye FITC. (A) Absorption spectra of unconjugated QD-PZ(aminoPEG$_3$)$_{10\%}$ (— black), QD-PZ(aminoPEG$_3$)$_{10\%}$- FITC mixture (--- blue), QD-PZ(aminoPEG$_3$)$_{10\%}$- FITC purified (— blue). (B) Absorption spectra of unconjugated QD-PZ(aminoPEG$_3$)$_{25\%}$ (— black), QD-PZ(aminoPEG$_3$)$_{10\%}$- FITC mixture (--- red), QD-PZ(aminoPEG$_3$)$_{10\%}$- FITC purified (— red) normalized at 598 nm.

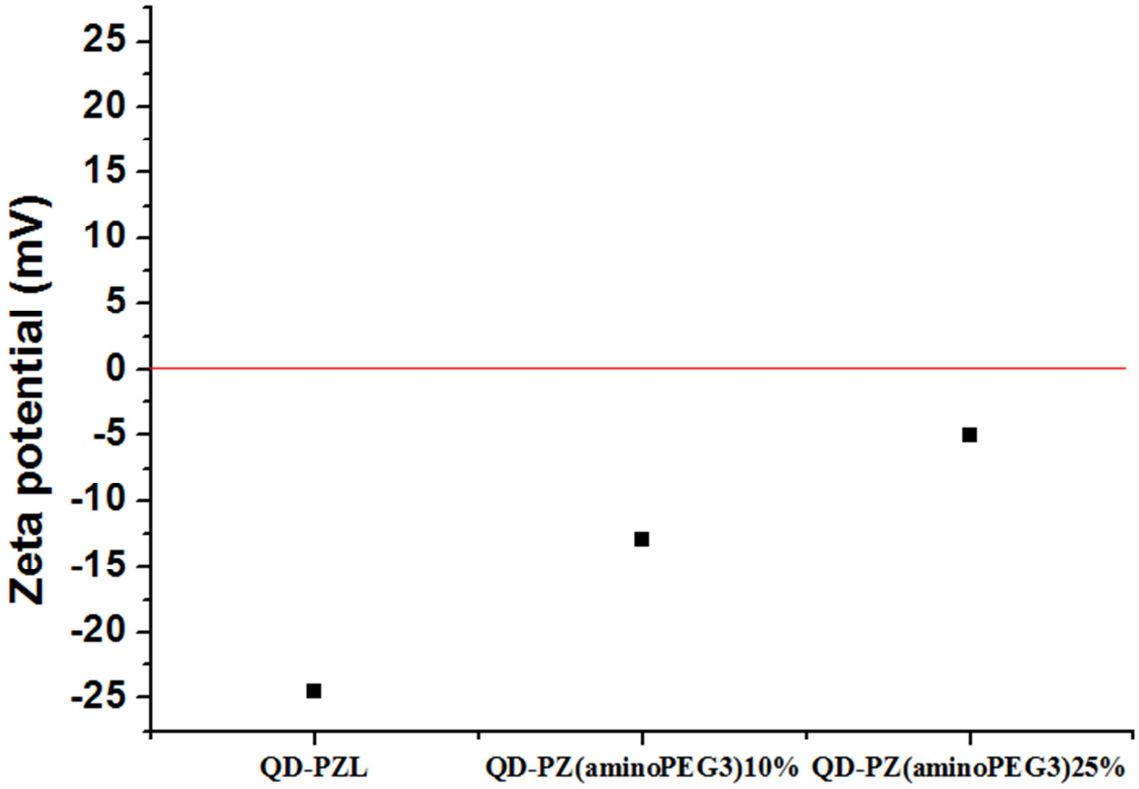

Figure 4 Zeta potentials of QD-PZL, QD-PZ(aminoPEG$_3$)$_{10\%}$, QD-PZ(aminoPEG$_3$)$_{25\%}$ particles respectively in water.

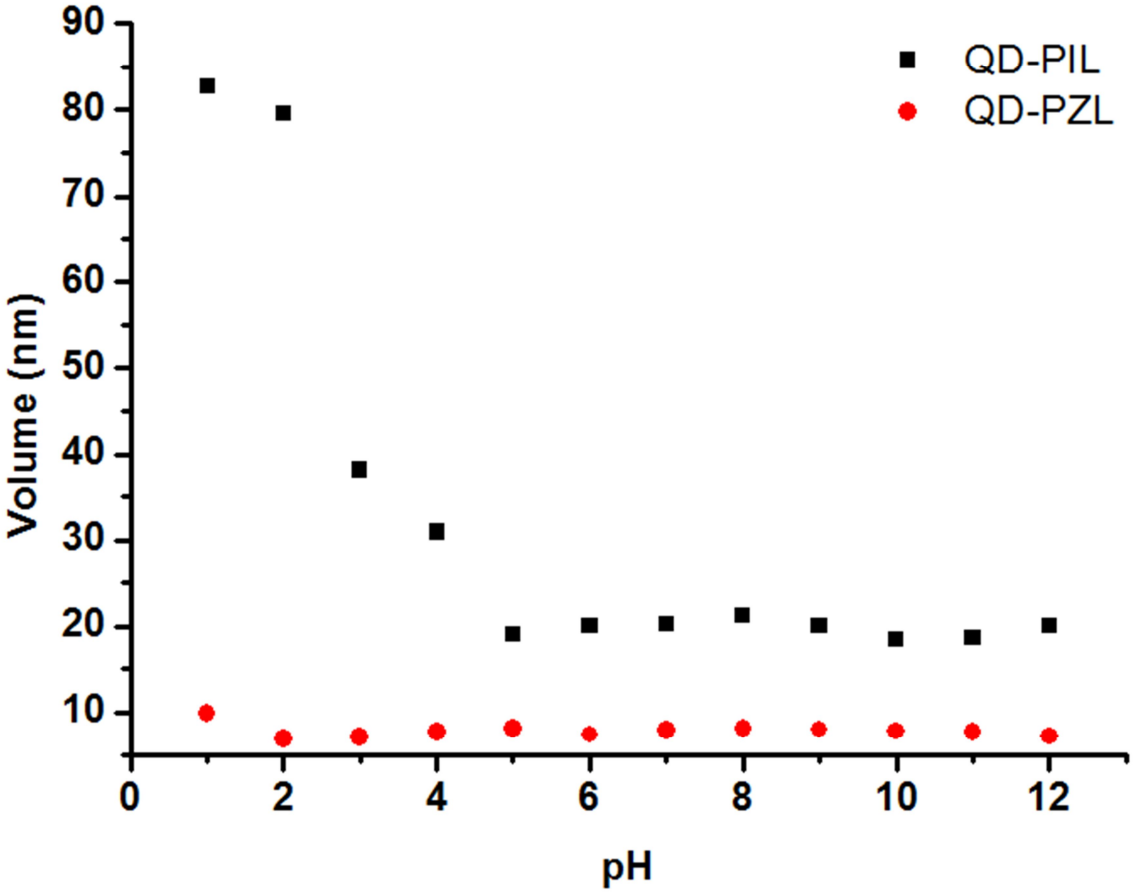

Figure 5 pH stability of QD-PZL and QD-PIL.

Fluorescent imaging of QD-PZL to Hela cells and nonspecific binding property. Non-biofouling is needed to reliable targeting and sensing applications involving QDs. To demonstrate the nonspecific binding of polyzwitterionic ligand coated QDs, we incubated Hela cells with various amine functional group modified QD-PZL and subsequently washed the Hell cells with phosphate-buffered saline (PBS). The fluorescence images of cells are shown in Figure 6. In case, QD-PZL without functional group, which wasn't conjugated with Folic acid, wasn't bound at folate receptor of Hela cells (Figure 6A). Otherwise, QD-PZL with conjugated folic acid shown the binding folate receptor of Hela cells, consistent with an increase in the amount of amines on the QD surface. The folate was conjugated to functional amine on the surface of QD-PZLs using EDC/NHS coupling chemistry. We incubated Hela cells with QDs (400 mg/ml) of modified functional amine number (0, 10, 25% of amine, respectively) for 12 h (Figure 6B, C).

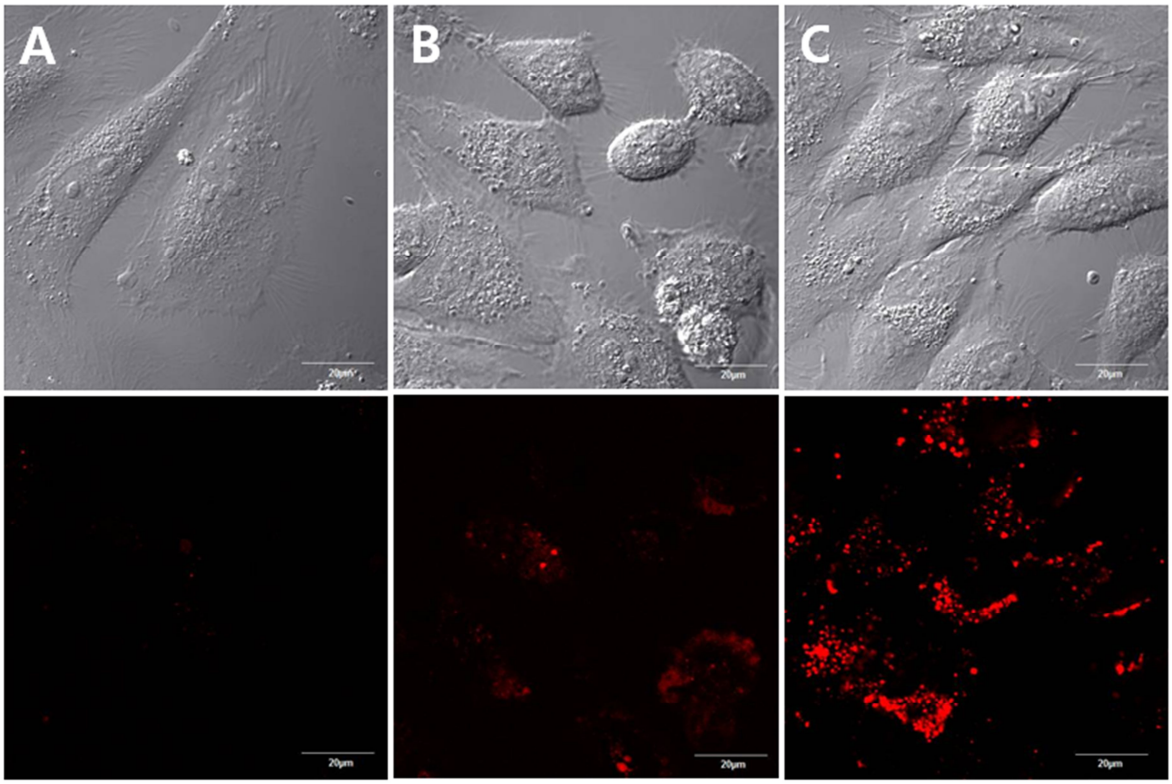

Figure 6 Fluorescent images of folate receptor of Hela cells labeled QD-PZL with folic acid. (A) Non-biofouling of polyzwitterionic ligand exchanged QDs without functional site on Hela cells. (B) Folate receptor targeted QD-PZ(aminoPEG$_3$)$_{10\%}$-FAs and (C) Folate receptor targeted QD-PZ(aminoPEG$_3$)$_{25\%}$-FAs, Fluorescent image of Hela cells with 488 nm excitation, 480 – 600 nm emission scan. All images are scaled to the same contrast with scale bar 20 um).

3. Summary

In this study, we demonstrated that Polyzwitterionic (MPDSAH) ligand-coated QDs were a promising materials for application of bio-imaging such as diagnosis. Our creation is comparable to the previously report for resisting the nonspecific adsorption of protein and highly stable condition. To demonstrate conjugation efficiencies of the amide bond on QDs, zwitterionic ligand coted QDs with functional amine were conjugated with FITC. To confirm coupling yield through knowledge of the extinction coefficients of the dye and QDs and measurement of the product absorption spectra.39 The number of FITC 521 nm dye molecules conjugated to the functional amine of QD-PZLs were concentrated to 20-fold excess molar ratio (dye/QDs) led to saturation coupling yield of 75% conjugated dye and 40% conjugated dye at QD-PZLs with 25% and 10% functional amine respectively.

To test the use of the Folate labeled QD-PZLs for biological imaging, where the cultured Hela cell lines folate receptors overexpressed on the surface of human cancer cells. In the results, we demonstrated the nonspecific binding to a human cell line as a zwitterionic ligand on QD surface without functional amine. And we demonstrated working of many amine function on QD surface.

In conclusions, we have examined that RAFT synthesized polyzwitterionic ligand is able to ligand exchange method for conjugation of QDs for stabilization in aqueous condition and to confirm working the functional amine on the QD surface. In this method, hydrophobic surface QDs were fabricated by ligand exchanging zwitterionic ligand which was a known non-biofouling polymer. This characteristic structure not only protects the QDs but also provides biological imaging applications.

4. Experimental

General Method. We purchased all chemicals from Sigma-Aldrich or Fischer Scientific Chemical Company, except stated in the following. The AIBN was purified by recrystallization from methanol at 40 ℃ and dried. Polymerization was started with polymerization radical initiator 2,2'-azobisisobutyronitrile (AIBN) and controlled with molecular weight controlling agent Reversible addition–fragmentation chain-transfer polymerization (RAFT). RAFT agent grows in a nearly uniform size. For each polymerization, 'Each monomer' ratio was varied while checking the polymer molecular weight and characteristics. All reactions were performed under Ar unless otherwise noted. NMR spectra were recorded on a Varian VNMRS 600 spectrometer with $CDCl_3$ and D_2O as a solvent. THF was distilled over Na/benzophenone before use. Toluene and DMF was distilled over CaH_2. Transmission electron microscopy (TEM) was performed on a JEM-1400 that made in JEOL, Japan having 120 kV acceleration voltages, 0.38 nm Lattice resolution, 0.20 nm point resolution, and EDS resolution 132 eV, to confirm aggregation per each step. Sample specimens were prepared by placing a drop of the solution on a carbon-coated Cu grid (200 mesh, EM science). After 30 min, the remaining solution on a grid was removed with a filter paper, and the grid was air-dried for 8 h. Dynamic light scattering (DLS) experiments were carried out on a BI-200SM equipped with a diode laser (637 nm, 4 mW). All DLS data were handled on a Dispersion Technology Software (Brookhaven Instruments). Optical density of the solutions was measured on a on a JASCO V-670 UV-Vis spectrophotometer equipped with a thermostat sample holder with a magnetic stirrer. % Transmittance at 580 nm was used to calculate the optical transmittance (O.T) of the solution by the following equation. $O.T = 1 - ((T_{buf} - T_{sol})/T_{buf})$ where T_{buf} was the % transmission of the buffer at 580 nm and T_{sol} was the % transmittance of the solution at the same wavelength. Confocal Laser Scanning Fluorescence Microscopy (CLSM) was performed on a FluoView 1000 Confocal Microscope (Olympus).

Synthesis of Acrylic NHS. Acrylic NHS is previous step compound used in synthesizing BHA and BPA. First, a solution of dicyclohexyl-carbodiimide (DCC) (5.145 g, 24.975 mmol) in 15 mL dry THF was added dropwise to a solution of Acrylic acid (1.50 g, 20.82 mmol) and N-hydroxysuccinimide (NHS) (2.865 g, 24.975 mmol) in 60 mL dry THF with stirring at 4 ℃. After dropwise, the solution was warmed to the room temperature and stirred 4 h. precipitates were removed by filtration, and evaporated in vacuo. Ethylacetate was added to precipitate additional by product, and the solution was filtered again. The solvent was evaporated and dissolved in either 10 mL anhydrous DMF or THF to create stock solution.

Synthesis of BOC Histamine Acrylate (BHA). A solution histamine dihydro-chloride (2.5 g, 13.59 mmol) in 50 mL DMF was added to aqueous solution of Sodium bicarbonate (50 mL, 0.3 M). Acrylic NHS prepared in previous synthesize was added dropwise with stirring at 4 ℃. After dropwise, the

solution was warmed to room temperature and monitored with silica TLC by ninhydrin stain for 12 h. The precipitates were removed by filter. The product was evaporated in vacuo and redissolved in 50 mL of DMF. Additional filter was needed and triethylamine (2.27 mL, 16.3 mmol) was added to the filtered solution. *Ditert*-butyl dicarbonate was added dropwise with stirring at 4 ℃ and the reaction was remained overnight at room temperature. Proper amount of water was added to separate DMF from crude solution, and the solution was extracted with $CHCl_3$ (4 × 20 mL). Magnesium sulfate was used to dry water, and the solvent removed in vacuo. The pure product was obtained by silica column (Change the ratio of ethyl acetate/hexanes gradient). ^{1}H NMR (600 MHz, $CDCl_3$) δ (ppm) 7.92 (s, 1H), 7.15 (s, 1H), 6.24 (dd, J_1 = 1.8 Hz, J_2 = 17.0 Hz, 1H), 6.10 (dd, J_1 = 9.8 Hz, J_2 = 17.0 Hz, 1H), 5.60 (dd, J_1 = 1.8 Hz, J_2 = 10.0 Hz, 1H), 3.61 (dt, 2H), 2.70 (t, 2H), 1.55 (s, 9H) .

Synthesis of BOC PEG Acrylate (BPA). *Ditert*-butyl dicarbonate (1.98 g, 9.09 mmol) was added dropwise to a solution of 4,7,10-trioxa-1,13-tridecanediamine (10.00 g, 45.45 mmol) in DCM (25 mL) with stirring at 4 ℃. After dropwise, the solution was warmed to room temperature and stirred overnight. The solution was worked up with water (3 × 20 mL) to remove unreacted reagent. Magnesium sulfate was used to dry water and solvent evaporated in vacuo. The cure product (2.53 g, 11.51 mmol) was dissolved in a mixture of sodium bicarbonate (13.3 mL, 0.3 M), and DMF (13.3 mL). To the solution, Acrylic NHS was added dropwise with stirring at 4 ℃. The reaction was monitored with silica TLC by ninhydrin stain for 2h. Proper amount of water was added to separate DMF from crude solution, and the solution was extracted with $CHCl_3$ (4 × 20 mL). Magnesium sulfate was used to dry water, and the solvent removed in vacuo. The pure product was obtained by silica column (Change the ratio of ethyl acetate/hexanes gradient). H-NMR was used to confirm the result of final product. ^{1}H NMR (600 MHz, $CDCl_3$) δ (ppm) 6.23 (dd, J1 = 2.0 Hz, J2 = 17.0 Hz, 1H), 6.10 (dd, J1 = 9.8 Hz, J2 = 17.0 Hz, 1H), 5.59 (dd, J1 = 2.0 Hz, J2 = 9.8 Hz, 1H), 3.66-3.45 (m, 14H), 3.20 (t, 2H), 1.82-1.75 (m, 4H), 1.42 (s, 12H).

Synthesis of 2-(Dodecylthiocarbonothioylthio)-2-methylpropanoic acid (TC)[41] TC was purchased from Aldrich and also synthesized by the literature method

Synthesis of TC-terminated poly(ethylene glycol) (PEG-CTA)[42] TC (7.2 g, 20 mmol) and oxalyl chloride (8.6 mL, 100mmol) were added into 40mL dry CH_2Cl_2 and stirred at room temperature until gas evolution stopped. Excess reagents were then removed under vacuum, and the residue was redissolved in 80 mL dry CH_2Cl_2, followed by addition of methoxy poly(ethylene glycol) (Mn = 2000 g/mol) (8 g, 4 mmol in 100mL dry CH_2Cl_2). The reaction was stirred for 24 h at room temperature and the mixture was concentrated before precipitation from an excess of cold Et_2O. The crude polymer obtained by filtration was purified by redisolving in CH_2Cl_2, precipitated in Et_2O, and dried under vacuum overnight. Yellow powder was obtained. ^{1}H NMR (600 MHz, $CDCl_3$) δ 4.25 (t, 2H), 3.64(m, 178H), 3.38 (s, 3H), 3.26 (t, 2H), 1.70 (s, 6H), 1.23-1.40 (m, 20H), 0.88 (t, 3H).

Polymerization. Stock solution of monomers BPA (45 mg, 0.125 mmol, in EtOAc), MPDSAH (36.5 mg, 0.125 mmol, in MeOH), BHA (66 mg, 0.250 mmol, in EtOAc), RAFT agent (20.7944 mg, 0.0088 mmol, in MeOH) were added in ampule. The solvent was removed in vacuo and AIBN (0.3 mg, 0.0018 mmol, in MeOH) were added with anhydrous methanol (1 mL). The ampule was subjected to 4 cycles of freeze-pump-thaw, and sealed under vacuum state using a butane torch. The ampule was heated at 70 ℃ in oil bath for overnight. Crude polymer was washed with hexane and minimum of mixture ethyl ether and methanol. 4 M HCl in dioxane solution was added to cleave the BOC protecting groups. After 1h deprotection, the HCl was removed in vacuo. The deprotected polymer was dissolved in water and a solution of NaOH in MeOH (1 M) was added dropwise to adjust the pH to be near 7-8. The solvent was removed in vacuo, and then the product was dissolved in water and the solution was filtered through a 0.2 um cellulose syringe filter. Polymerization was repeated while varying monomer ratio, BPA : MPDSAHIS : BHA = 1 : 4 : 5.

Ligand Exchange with PZL. QDs (5 mg) were precipitated using MeOH and brought into 100 μL of $CHCl_3$. The QD stock solution was mixed with polymer of PZL (100 mg) and stirred for 30 min at RT after which 100 μL of water was added followed by stirring for an additional 120 min at 50 ℃ in oil bath. QD-PZLs in solvent were precipitated by the addition of ethanol (100 μL), $CHCl_3$ (100 μL), and excess hexanes for washing. The samples were centrifuged at 4000 rpm for 2 min. The clear supernatant was discarded, and the pellet dried in vacuo, followed by the addition of PBS (500 μL, pH 7.4). The aqueous sample was then filtered through a 0.2 μm syringe filter before use.

Measure M_w with Static Light Scattering (SLS). We used SLS to measure molecular weight of polymer rather than GPC because the zwitterionic polymer was dissolved in only water. SLS is technique measuring the intensity of scattered light to obtain the average molecular Wight M_w of a polymer. We obtained refractive index value dc/dn = $-1.773e^{-02}$ from BI-DNDC technique measured each sample stocks (1~5 mg/mL). Following we obtained the molecular weight M_w=2.8×10^4 g/mol from Zimm plot technique.

In vitro assay Hela cell Labeling. Hela cells were propagated in Dulbecco's Modified Eagle Medium (DMEM) supplemented with FBS (Fetal Bovine Serum 10%) and PS (Penicillin/Streptomycin 1%). Then the cultured cells were trypsinized and resuspended in the DMEM at a concentration of about 2×10^4 cells/ml. The cell suspension (500 uL) was transferred to each Chambered Coverglass (8 units). After 24 h of incubation, the cells were carefully rinsed with PBS. For each Chamber, the DMEM medium (500 uL) and the folic acid conjugated QDs (400 ug/mL) were added and incubated for 12 h. After 12 h, the QD-PZ(aminoPEG$_3$)-FAs labeled cells were carefully rinsed with PBS to remove unbounded QD-PZ(aminoPEG$_3$)-FAs, and fresh DMEM medium (500 uL) was added to each chamber for cellular viability. The fluorescent imaging of live Hela cells was performed on an FV1000 with SIM and Live fluorescence microscope (Olympus).

Compound 4

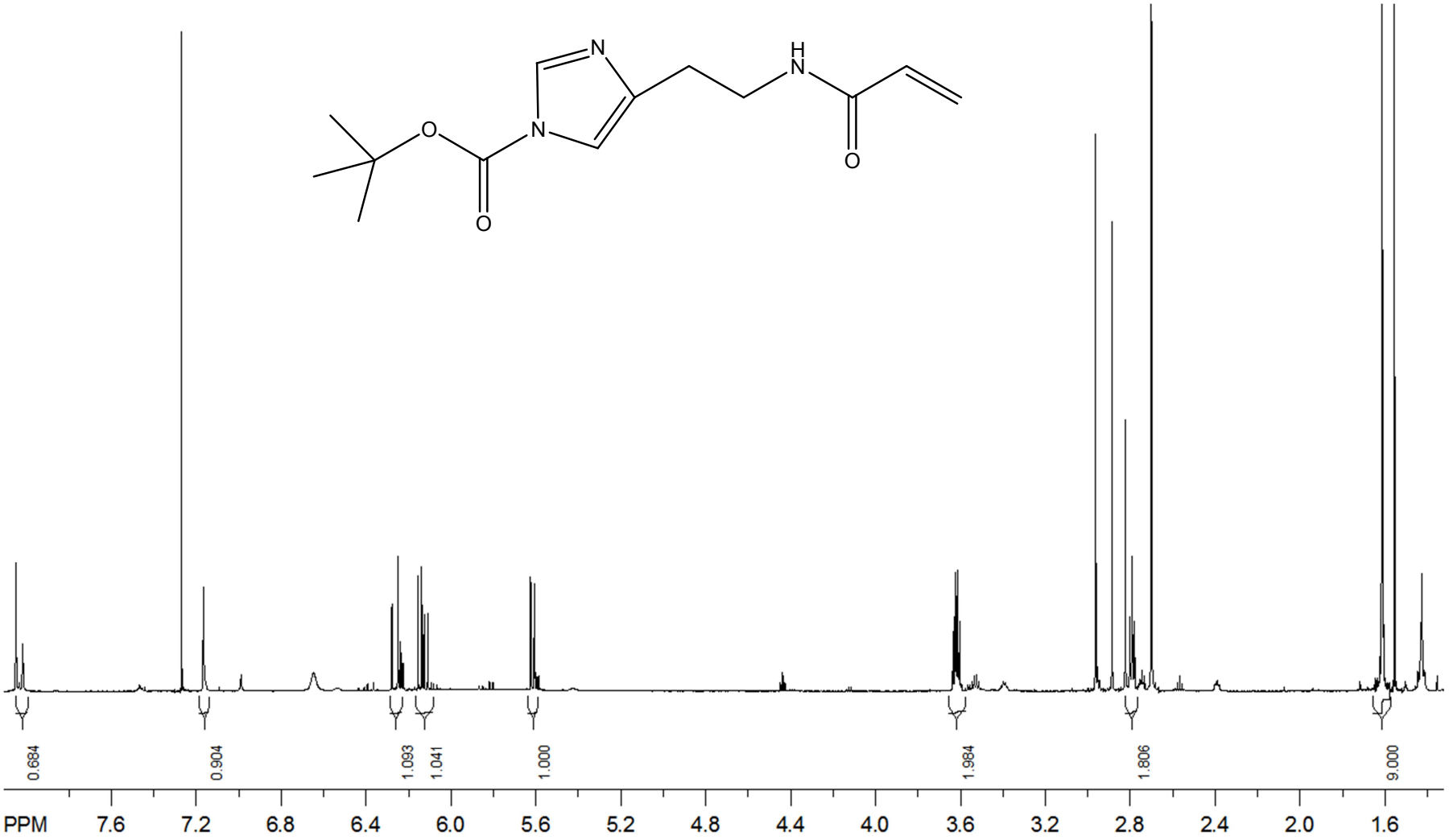
N
H
N
O
N
O
O
0.684
0.904
1.093
1.041
1.000
1.984
1.806
9.000
PPM
7.6
7.2
6.8
6.4
6.0
5.6
5.2
4.8
4.4
4.0
3.6
3.2
2.8
2.4
2.0
1.6

Compound 6

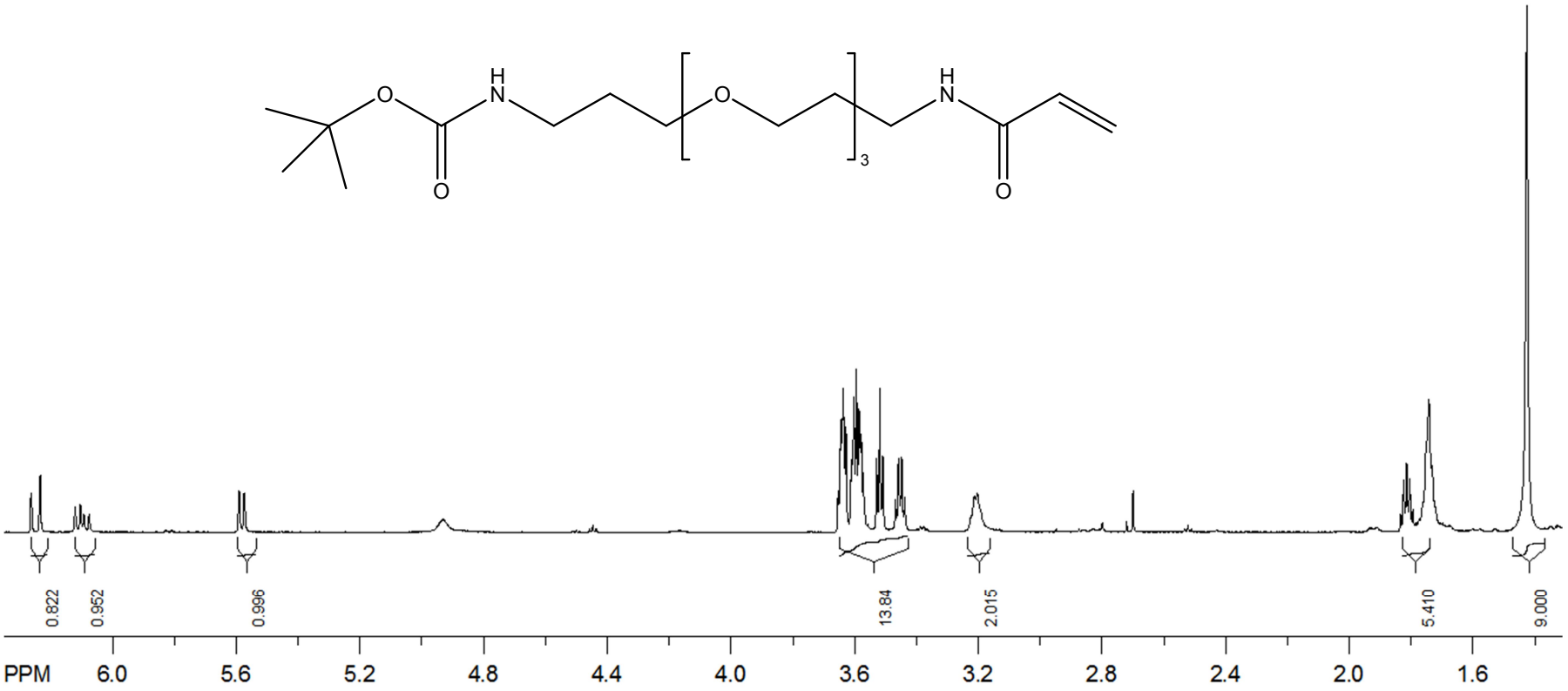

Figure 7 ^{1}H-NMR spectrum of compound 4, 6.

Reference

1. Erathodiyil, A.; Ying, J. Y. *Acc. Chem. Res.* **2011**, 44, 925-935.

2. Liu, W.; Greytak, A. B.; Lee, J.; Wong, C. R.; Park, J.; Marshall, L. F.; Jiang, W.; Curtin, P. N.; Ting, A. Y.; Nocera, D. G.; Fukumura, D.; Jain, R. K.; Bawendi, M. G. *J. Am. Chem. Soc.* **2010**, 132, 472-483.

3. Dabbousi, B. O.; Rodriguez-Viejo, J.; Mikulec, F.V.; Heine, J. R.; Mattoussi, H.; Ober, R.; Jensen, K.F.; Bawendi, M. G. *J. Phys. Chem. B* **1997**, 101, 9463-9475.

4. Zimmer, J. P.; Kim, S.-W.; Ohnisi, S.; Tanaka, E.; Frangioni, J. V.; Bawendi, M. G. *J. Am. Chem. Soc.* **2006**, 128, 2526-2527.

5. Bruchez, M., Jr; Moronne, M.; Gin, P.; Weiss, S.; Alivisatos, A. P. *Science* **1998**, 281, 2013-2016.

6. Peng, Z. A.; Peng, X. *J. Am. Chem. Soc*. **2001**, 123, 183-184.

7. Dahan, M.; Levi, S.; Luccardini, C.; Rostaing, P.; Riveau, B.; Triller, A. *Science* **2003**, 302, 442-445.

8. Michaluk, P.; Mikasova, L.; Groc, L.; Frischknecht, R.; Choquet, D.; Kaczmarek, L. *J. Neurosci.* **2009**, 29, 6007-6012.

9. Iyer, G.; Michalet, X.; Chang, Y. P.; Pinaud, F. F.; Matyas, S. E.; Payne, G.; Weiss, S. *Nano Lett.* **2008**, 8, 4618-4623.

10. Chen, Y.; Thakar, R.; Snee, P. T. *J. Am. Chem. Soc.* **2008**, 130, 3744-3745.

11. Cho, W. K.; Kong, B.; Choi, I. S. *Langmuir* **2007**, 23, 5678-5682.

12. Poly(ethylene glycol) Chemistry: Biotechnical and Biomedical Applications; Harris, J. M., Ed.; Plenum Press: New York, 1992.

13. Ma, H.; Hyun, J.; Siller, P.; Chilkoti, A. *Adv. Mater.* **2004**, 16, 338-341.

14. Ma, H.; Wells, M.; Beebe, T. P.; Chilkoty, A. *Adv. Funct. Mater.* **2006**, 16, 640-648.

15. Ma, H.; Li, D.; Sheng, X.; Zhao, B.; Chikoti, A. *Langmuir* **2006**, 22, 3751-3756.

16. Jo, S.; Park, K. *Biomaterials* **2000**, 21, 605-616.

17. Prime, K. L.; Whitesides, G. M. *J. Am. Chem. Soc.* **1993**, 115, 10714-10721.

18. Ostuni, E.; Chapman, R. G.; Liang, M. N.; Meluleni, G.; Pier, G.; Ingber, D. E.; Whitesides, G. M. *Langmuir* **2001**, 17, 6336-6343.

19. Kane, R. S.; Deschatelets, P.; Whitesides, G. M. *Langmuir* **2003**, 19, 2388-2391.

20. Herrwerth, S.; Eck, W.; Reinhardt, S.; Grunze, M. *J. Am. Chem. Soc.* **2003**, 125, 9359-9366.

21. Lee, B. S.; Lee, J. K.; Kim, W.-J.; Jung, Y. H.; Sim, S. J.; Lee, J.; Choi, I. S. *Biomacromolecules* **2007**, 8, 744-749.

22. Ostuni, E.; Chapman, R. G.; Holmlin, R. E.; Takayama, S.; Whitesides, G. M. *Langmuir* **2001**, 17, 5605-5620.

23. Herold, D. A.; Keil, K.; Bruns, D. E. *Biochem. Pharmacol.* **1989**, 38, 73-76.

24. Harder, P.; Grunze, M.; Dahint, R.; Whitesides, G. M.; Laibinis, P. E. *J. Phys. Chem. B* **1998**, 102, 426-436.

25. Shen, M. C.; Martinson, L.; Wagner, M. S.; Castner, D. G.; Ratner, B. D.; Horbett, T. A. *J. biomater. Sci. Polym. Ed.* **2002**, 13, 367-390.

26. Li, L. Y.; Chen, S. F.; Jiang, S. Y. *J. Biomater. Sci. Polym. Ed.* **2007**, 18, 1415-1427.

27. Gaberc-Porekar, V.; Zore, I.; Podobnik, B.; Menart, V. *Curr. Opin. Drug Discov. Devel.* **2008**, 11, 242-250.

28. Jiang, S.; Cao, Z. *Adv. Mater.* **2010**, 22, 920-932.

29. Jeon, S. I.; Lee, H.; Andrade, D.; Gennes, P. G. de *J. Colloid Interface Sci.* **1991**, 142, 149-158.

30. McPherson, T.; Kidane, A.; Szleifer, I.; Park, K. *Langmuir* **1998**, 14, 176-186.

31. Luk, Y.-Y.; Kato, M.; Mrksich, M. *Langmuir* **2000**, 16, 9604-9608.

32. Estephan, Z. G.; Jaber, J. A.; Schlenoff, J. B. *Langmuir* **2010**, 26(22), 16884-16889.

33. Efremova, N. V.; Sheth, S. R.; Leckband, D. E. *Langmuir* **2001**, 17, 7628-7636.

34. West, S. L.; Salvage, J. P.; Lobb, E. J.; Armes, S. P.; Bilingham, N. C.; Lewis, A. L.; Hanlon, G. W.; Lloyd, A. W. *Biomaterials* **2004**, 25, 1195-1204.

35. Zwaal, R. F. A.; Comfurius, P.; Van Deenen, L. L. M. *Nature* **1977**, 268, 358-360.

36. Chang, Y.; Chen, S.; Zhang, Z.; Jiang, S. *Langmuir* **2006**, 22, 2222-2226.

37. Zhang, Z.; Chen, S.; Jiang, S. *Langmuir* **2006**, 22, 10072-10077.

38. Zhang, Z.; Chen, S.; Chang, Y.; Jiang, S. *J. Phys. Chem. B* **2006**, 110, 10799-10804.

39. Han, H. S.; Devaraj, N. K.; Lee, J.; Hilderbrand, S. A.; weissleder, R.; Bawendi, M. G. *J. Am. Chem. Soc.* **2010**, 132, 7838-7839.

40. Naoto, A.; Bungo, O.; Hideharu, M.; Takeshi, E. *Syn. Lett.* **2006**, 4, 636-638.

41. Lai, J. T.; Filla, D.; Shea, R. *Macromolecules* **2002**, 35, 6754–6756.

42. Huang, C.-Q.; Pan, C. Y. *Polymer* **2010**, 22, 5115–5121.

Acknowledgement